

Published in final edited form as:

Trends Analyt Chem. 2016 June ; 80: 311–320. doi:10.1016/j.trac.2015.06.013.

Size-exclusion chromatography of metal nanoparticles and quantum dots

Leena Pitkänen and André M. Striegel*

National Institute of Standards and Technology, Chemical Sciences Division, 100 Bureau Drive, MS 8392, Gaithersburg, MD 20899, USA

Abstract

This review presents an overview of size-exclusion chromatographic separation and characterization of noble metal nanoparticles (NPs) and quantum dots (QDs) over the past 25 years. The properties of NPs and QDs that originate from quantum and surface effects are size dependent; to investigate these properties, a separation technique such as size-exclusion chromatography (SEC) is often needed to obtain narrow distribution NP populations that are also separated from the unreacted starting materials. Information on the size distributions and optical properties of NPs have been obtained by coupling SEC to detection methods such as ultraviolet-visible and/or fluorescence spectroscopy. Problems associated with the sorption of NPs and QDs onto various SEC stationary phases, employing both aqueous and organic eluents, are also discussed here.

Keywords

size-exclusion chromatography; characterization; metal nanoparticles; quantum dots

1 Introduction

Nanoparticles (NPs) are particles of any shape having a size, in at least one dimension, between 1 nm and 100 nm. Small NPs (< 10 nm), which are also referred to as nanoclusters or nanocrystals, are defined as clusters of atoms with atom numbers ranging anywhere from 3 to 10^7 . In theory, there are two ways to generate NPs: To cleave the bulk material into nanoscopic material (although this is rarely done experimentally), or to condense atoms into clusters and NPs. Due to the nanometer range size of NPs, their properties have features representative both of atoms and of bulk solid- or liquid-state materials. The unique properties of NPs originate from quantum effects and surface effects, both of which are size-dependent. The investigation of quantum effects focuses on how electronic and structural NP properties such as ionization potentials, binding energies, chemical reactivity, crystallographic structure, melting temperatures, or optical properties vary as a function of particle size. Surface effects are related to the fraction of the atoms at the surface of NPs. A broader introduction to NP synthesis and properties can be found in various excellent books

*Corresponding author. Tel. 301-975-3159; fax: 301-977-0685, andre.striegel@nist.gov (A.M. Striegel).

and review articles on the topic, such as the review by Roduner [1] and the book by Kreibig and Vollmer [2].

Among metal NPs, gold (Au) and silver (Ag) NPs are the most widely studied due to their numerous applications as sensors, nanocarriers, and in cosmetics [3–5], among others. The applicability of these NPs stems from their visible absorption bands, straightforward method of synthesis (with high degree of size and shape control), stability, biological compatibility, and easy functionalization with various (bio)molecules. Nanocrystals composed of semiconductor materials, and which exhibit quantum mechanical properties, are also known as quantum dots (QDs) and include materials consisting of cadmium sulfide (CdS), cadmium selenide (CdSe), cadmium telluride (CdTe), and zinc sulfide (ZnS). QDs have applications in, *e.g.*, biological imaging and labeling, lasers, light-emitting diodes (LEDs), and solar cells [6–8]. Both metal NPs and QDs are usually stabilized or coated to prevent aggregation and to modify their surface properties for targeted applications. The size of Ag and Au NPs ranges from a couple of nanometers (nanoclusters) to several tens of nanometers. In general, QDs are in the range of nanoclusters smaller than 10 nm.

As indicated by the first paragraph of this **Introduction**, many properties of both metal NPs and QDs are size-dependent. Thus, study of the size-dependent properties of NPs requires narrow size-dispersity, high purity samples. Generally, these types of samples are obtained by fractionation of the bulk sample employing, most commonly, size-exclusion chromatography (SEC). This review focuses on the SEC analysis of different metal NPs and QDs by attempting to summarize the past 25 years of work in this area. During this period, research on all aspects of NPs has increased tremendously. In addition to summarizing the existent literature on SEC separation and characterization of NPs and QDs, our aim is to discuss the challenges related to their SEC separation and detection. Because we intend this review for a broad audience, before discussing the NP applications of SEC we give a short introduction to this separation technique and to the associated detection methods employed in NP analyses.

2 SEC instrumentation for characterization of metal NPs and QDs

2.1 General principles of SEC, column types, and mobile phases

SEC is a column liquid chromatographic technique commonly used for the separation of macromolecules in solution. Usually, SEC columns are packed with small, rigid porous particles of size ranging from 3 μm to 20 μm and pore size from 50 \AA to 10^7 \AA . SEC separates molecules according to their size in solution or, to be more specific, their hydrodynamic volume. The larger molecules in a sample elute before the smaller ones because larger molecules either enter fewer pores or sample a smaller pore volume of the column packing material (depending on whether the column is of a mixed bed or individual pore size type). Unlike other chromatographic techniques which rely mainly on enthalpic interactions between stationary phase and analytes, SEC is primarily an entropy-controlled process; the separation is based on exclusion of the molecules from the pores of the SEC stationary phase and ideally, no interaction between the analytes and stationary phase occurs [9,10]. In practice, this entropic dominance is sometimes difficult to achieve and, as we shall

see, the separation of two gold NPs with different shapes could be obtained only when two mechanisms, size-exclusion and adsorption, were combined within a single separation.

SEC column stationary phases are commonly either polymer-based (*e.g.*, styrene/divinylbenzene) or silica-based. A wide selection of mobile phases (both aqueous and organic, depending on the procedure employed for NP or QD synthesis) can be used with either type of stationary phase. Indeed, many different combinations of SEC columns and mobile phases have been employed for NP and QD analysis, as summarized in Table 1 (in this review, for the sake of simplicity, SEC in aqueous solution will be referred to as “aqueous SEC”, while SEC employing organic eluents will be referred to as “organic SEC”). As can be seen in Table 1, both polymer- and silica-based columns (note that Nucleosil is a silica column, whereas Nucleogel and PL/PLgel columns are polymer-based) are employed in aqueous solution, whereas polymer-based columns are commonly used only with organic solvents.

The most significant challenge in the SEC analysis of metal NPs and QDs is their adsorption to the column packing material. Adsorption can cause several problems in SEC analysis of NPs and QDs. Firstly, if adsorption occurs, due to incomplete analyte recovery (*i.e.*, the amount of material that elutes from the columns is less than the amount injected), results will not be quantitative. Secondly, the hydrodynamic diameters obtained by the calibration of column(s) using size standards will be biased, because of the shift in retention volumes caused by analytes interacting with the column stationary phase. Researchers have attempted to overcome these adsorption problems by employing columns with large pore size (small surface area) and by modifying the mobile phase with additives that reduce the enthalpic interactions between the NPs and the column stationary phase. As can be seen in Table 1, mobile phase additives include surfactants, molecules that have been used as coating/stabilizing agents for the NPs, and modifiers containing the cations from which the NP is composed of (*e.g.*, cadmium perchlorate for the analysis of CdS).

2.2 Detection

As can be seen in Table 1, all SEC studies on metal NPs and QDs employ ultraviolet-visible (UV-Vis) spectroscopy (either single- or multiple-wavelength) as a detection method. For example, Au NPs have a surface plasmon band at 520 nm, hence the commonality of this wavelength for detection of these NPs. In addition to UV-Vis, other detectors employed for NP detection include differential refractive index (DRI), fluorescence (FL), and conductivity. Because the sensitivity of DRI is rather low compared to that of UV, the latter has mainly been employed for detection of NPs, whereas the former has been useful in detection of residual non-absorbing chemicals from the NP synthesis. FL detection has been used in the investigation of NP and QD photoluminescence, as we shall see in the following sections. Transmission electron microscopy (TEM), which is the most common size-determination technique for NPs and QDs, has been used off-line from SEC, to determine the sizes of each of the fractions eluted from the chromatographic column. In some cases, size results from TEM were compared to results from SEC obtained by calibrating the columns using well-characterized size standards (either NP standards or polymer-based standards). Results from these comparisons are discussed in Sections 3 and 4.

3 Aqueous SEC of Au NPs and QDs

3.1 Gold nanoparticles (Au NPs)

The majority of research on aqueous SEC of metal nanoparticles has been conducted using Au NPs. The first reports on the SEC characterization of colloidal Au NPs were published on 1993 and 1994 by Siebrands *et al.* [11] and by Fischer and Giersig [12]. Those studies demonstrated for the first time how SEC can be employed for the separation and size characterization of Au NPs with a size range of 2.9 nm to 20 nm. A plot of the logarithm of particle size (as determined by TEM) as a function of SEC elution time was linear, supporting the notion that the NP separation was based on a size-exclusion mechanism. The SEC columns used in those studies had a large particle size, ranging from 15 μm to 25 μm (Nucleosil 500 and Nucleosil 1000 C4, respectively), because it was found that Au NPs adsorbed irreversibly onto silica columns of particle size lower than 15 μm . Already we see that the first studies on aqueous SEC of Au NPs indicated the existence of the adsorption problem that has hindered the widespread use of SEC for accurately characterizing NPs in aqueous solution.

Aqueous SEC was also used by Wilcoxon *et al.* [13], who employed SEC coupled with UV-Vis and fluorescence detection to purify small gold nanoclusters and investigate their photoluminescence. Novak *et al.* [22] used SEC/UV ($\lambda_0 = 525 \text{ nm}$) for separating phenylethynyl-bridged Au NP dimers and trimers from excess monomer particles. The sizes (or more precisely, the aggregate type and proportion in each separated fraction) of the SEC-separated Au NPs were determined off-line, using TEM. Before attempting the separation of these NPs, the SEC system was tested by injecting a mixture of pure 10 nm, 20 nm, and 30 nm Au NPs and a mixture of 10 nm and 30 nm Au NPs onto the columns. The 30 nm particles were meant to mimic the trimers of 10 nm-sized monomers. The resolution between 10 nm and 30 nm particles was 0.8. This resolution was higher than that obtained when injecting the phenylethynyl-bridged Au NPs, where a resolution of 0.5 was measured between monomers and trimers. This difference in resolution is not surprising, given that the monomeric components in the trimers are arranged in a triangular, rather than straight line, fashion, where the former geometry occupies a smaller hydrodynamic volume than does the latter. In the separations, two silica-based SEC columns (500 Å and 350 Å) were used in series with 40 mmol L⁻¹ sodium dodecyl sulfate (SDS) in water as mobile phase.

The majority of papers on aqueous SEC of Au NPs has been written by Wei and Liu, and Liu [14–21,23,24,42]. These authors' early work focused on finding the analytical conditions for separation of Au NPs and gold nanorods [14–16]. In said studies, different mobile phase additives (in water) were evaluated to find an eluent that would prevent the irreversible adsorption of Au NPs (citrate stabilized and hexadecyltrimethylammonium bromide (CTAB) stabilized) to the SEC column packing material. The mobile phase additives tested included SDS, an anionic surfactant, at varying concentrations; a mixture of SDS and Brij-35, a neutral surfactant; sodium chloride; and sodium citrate. For the separation, both a polymer-based (styrene/divinylbenzene) and a silica-based column were evaluated. The authors found that, when either NaCl or sodium citrate were used as mobile phase additives, the Au NPs both aggregated with themselves and adsorbed onto either

column packing material. The addition of surfactants appeared to enable the separation of Au NPs on both types of column. According to the authors, SDS acted to prevent adsorption of the analytes onto the columns by both increasing the negative charge of the packing material and by changing the charge of the NPs from positive to negative. Adsorption is thus prevented by charge-charge repulsion between analyte and stationary phase, i.e., through ion-exclusion effects. Conversely, Brij-35 was added to increase separation resolution between the spherical and rod shaped analytes. It was postulated that the neutral Brij-35 replaced some of the charged SDS on the NP surface, decreasing the negative charge on the NPs and, thus, leading to a controlled increased adsorption of NPs onto the stationary phase in a size- and/or shape-dependent manner. The separation process was thus believed to be governed both by size-exclusion and adsorption mechanisms (Figure 1). In all of these studies, elution of Au NPs was monitored employing UV-Vis detection; it should be noted that observations regarding Au NP elution using various SEC analysis conditions were based on the differences in UV peak areas. Thus, the results obtained from all studies were only qualitative; the absolute Au NP concentrations eluted from the columns were not determined. The sizes of Au NPs used in these studies were determined using TEM.

Later studies from the same group report the use of aqueous SEC for separation and size characterization of Au NPs synthesized using various procedures [17,18,24]. SEC was also employed for stability studies of Au NP solutions [19–21]. A polymer-based (styrene/divinylbenzene) column and 10 mmol L⁻¹ SDS mobile phase were used in all of these studies. Size information on the studied Au NPs was obtained by calibrating the column using commercial Au NP standards with known diameters ranging from 12 nm to 79 nm. The elution of Au NPs was monitored using UV-Vis detection at $\lambda_0 = 520$ nm, which, as mentioned earlier, is the surface plasmon band of spherical Au NPs.

3.2 Quantum dots (QDs)

Although aqueous SEC, in the context of metal NP characterization, has mainly been employed for Au NPs, it has also been used for separation of polyphosphate-stabilized semiconductor particles of CdS [12,25–29] and ZnS [27]. The relatively short SEC analysis time enables characterization of rapidly growing colloidal species in solution, and allows studies on the stability and growth mechanism of semiconductor particles. For SEC analysis of these particles, the eluent contained both polyphosphate (also used as stabilizer of semiconductors in solution) and either cadmium perchlorate (for CdS) or zinc perchlorate (for ZnS). Narrow dispersity CdS and ZnS particles, the diameters of which were determined using TEM, were employed to calibrate the SEC columns with respect to particle diameter.

Although SEC was successfully employed for separation and size characterization of semiconductor particles in aqueous solution, concentration-dependent adsorption of NPs onto the SEC columns was observed, as indicated by a comparison of the UV peak areas obtained using different CdS concentrations [28]. It was found that the adsorption problem was more severe when NP concentration exceeded a certain molarity (>5 mmol L⁻¹ for CdS). In addition to adsorption, at CdS concentrations higher than 5 mmol L⁻¹ retention times increased due to a decrease in the thickness of the electrical double layer surrounding

the NPs. It should be noted that the adsorption phenomenon was found to be both irreversible and reversible, with the latter recognized by an increase in baseline drift as a function of elution time, ascribed to the release of semiconductor particles adsorbed onto the stationary phase. This adsorption activity was shown to be lower when the stationary phase was already coated by CdS (i.e., after several injections of a QD sample onto a new column) than for columns with an uncoated stationary phase.

In a later study, Trapiella-Alfonso *et al.* characterized CdSe and CdSe/ZnS QDs using a Superdex 200 SEC column [30]. Detection techniques included UV-Vis, FL, and inductively coupled plasma mass spectrometry (ICP-MS). Element-specific ICP-MS detection allowed determination of column recoveries (see Section 5 for further discussion of this last point).

4 Organic SEC characterization of NPs

4.1 Gold and silver nanoparticles (Au and Ag NPs)

In the first report on the use of SEC in organic solution for Au NP analysis, the photoluminescence of small Au nanoclusters synthesized in inverse micelles was studied by SEC coupled to photodiode array (PDA) and fluorescence detectors using tetrahydrofuran (THF) as eluent [13]. Later studies of Wilcoxon *et al.* [31–34] include the purification and investigation of the size distribution, optical properties, and stability of Au and Ag nanoclusters with SEC in toluene containing 0.01 mol L⁻¹ dodecane thiol. In these studies, the columns were calibrated for hydrodynamic radius (R_H) using polystyrene standards and linear alkanes. As pointed out by the authors [31], the benefit of SEC over TEM as a size determination method for metal nanoclusters is that, by SEC, the total cluster size is obtained (core + shell), whereas TEM sees only the inorganic core. By using both techniques, SEC and TEM, the size of the shell can be estimated by subtracting the core size obtained from TEM from the total cluster size obtained from SEC. An overlay of the SEC chromatograms of Au nanoclusters with different alkanethiol capping agents (C₆SH, C₁₀SH, C₁₄SH) is shown in Figure 2. The size of the Au core was 2.0 nm, as determined by high resolution TEM. The sizes obtained for alkanethiol shells varied slightly depending on the SEC column used (PL 1000 or PL 500). In general, the sizes determined with SEC were consistent with the assumption that every 4 carbon atoms added contribute an ≈ 8 Å increase in size to an alkanethiol.

Because the low resolution of conventional SEC can limit its applicability in nanomaterial separations, where the size difference between closely eluting species is very small, Al-Somali *et al.* [35] employed alternate-recycling SEC (also known as recycle SEC; see Section 15.3 of ref. [9]), which improved resolution in the separation of Au NPs capped with alkanethiols as compared to conventional SEC. In alternate-recycling SEC, the eluate from the first SEC column is directed to a second column (identical to the first one) via a low-volume, high-speed valve. The eluate from the second column is then transported back to the first column. This recycling process increases the effective column length and, thus, increases the resolution of species with only a small size difference between them. Figure 3 demonstrates the increase in resolution as a function of increasing cycle number obtained in alternate-recycling SEC. The resolution of individual species in a broad dispersity Au NP sample clearly increases as a function of cycle number. This can be seen by comparing

Figure 3a), in which the SEC chromatogram of a Au NP sample is shown after the second cycle, to Figure 3b), in which an SEC chromatogram of the same sample is shown after cycle number 8. Also seen in Figure 3b) is that the chromatograms from four injections overlay nicely upon one another, indicating that the recycle SEC system is both stable and reproducible for this Au NP sample at the analysis conditions used. Figure 3c) shows how resolution improves with increasing cycle number.

To date, the only report on the SEC characterization of Ag nanoclusters appears to be that by Wilcoxon *et al.* [32]. Ag nanoclusters were prepared by an inverse micelle technique in organic solvents and separated with SEC using 0.01 mol L^{-1} dodecanethiol in toluene as eluent. The aim of the study was to compare differences in the optics of Au and Ag nanoclusters arising from the different energies of the inter-band transition onsets of these two metals. The spectra of separated nanoclusters were recorded with a PDA detector, and the sizes of the Ag nanoclusters were obtained using the same calibration curve, constructed with linear alkanes and polystyrene standards, as described in the previous section for the size determination of Au nanoclusters. Results showed how both broadening and red shift of the absorbance spectrum occurred for Ag nanoclusters with decreasing cluster size, while for Au nanoclusters broadening was accompanied by blue shifting as a function of decreasing cluster size.

4.2 Quantum dots

The first studies on SEC of semiconductor particles in organic solvents date back to the early 1990s, when the first report on the separation of CdS nanocrystals was published by Fischer *et al.* [27]. There, it was demonstrated that SEC of CdS QDs stabilized with alkanethiols, in THF containing 1 mmol L^{-1} $\text{Cd}(\text{ClO}_4)_2$ + 1 mmol L^{-1} dodecanethiol, is feasible. Later studies by Wilcoxon and Provencio [37], Wang *et al.* [39], and Kruger *et al.* [36,38] have shown how SEC reveals various characteristics and size-dependent properties of CdSe and CdSe/ZnS core/shell nanocrystals, as described below.

Wilcoxon and Provencio [37] used SEC in THF employing three on-line detectors, fluorescence, diode array detection, and differential refractometry, for separation of both CdSe and CdSe/ZnS QDs and to investigate their size-dependent optical and chemical properties. SEC column calibration was not used for determination of hydrodynamic size, contrary to what had been done in earlier studies on Au NPs by this group, due to specific chemical interactions between the QDs and the column material (styrene/divinylbenzene), interactions which violated the ideal SEC separation mechanism. Rather, off-line dynamic light scattering (DLS) was used for size determination of CdSe and CdSe/ZnS QDs. Although size could not be determined directly by SEC, chromatographic analysis allowed isolation of the discrete size populations present, with the various on-line detectors providing insight into the optical properties of the individual fractions.

Krueger *et al.* [36,38] were able to employ SEC with toluene containing 0.1 mol L^{-1} trioctylphosphine for the hydrodynamic size determination of polystyrene- and alkythiol-coated CdSe nanocrystals. Polystyrene standards were used for size calibration of the SEC column. Sizes were also determined with TEM, with results from both methods consistent for nanocrystals with sizes ranging from $\approx 2.5 \text{ nm}$ to $\approx 4.0 \text{ nm}$. The successful SEC

separation of alkylthiol-coated CdSe nanocrystals, however, required complete capping for both Cd and Se atoms to eliminate particle-column interactions. An additional aim of this study was to investigate the change in the length of polystyrene chains when attached to CdSe versus unbound [36]. It was found that polystyrene linked to a metal core at full coverage (full coverage was defined by the maximum NP size measured by SEC) assumes a brush conformation and is 44 % longer than is the unbound polymer in solution. Figure 4a) illustrates how the total hydrodynamic diameter (HD) is defined as the sum of the core diameter (D_c) and two shell thicknesses (T_{shell}). As mentioned earlier, the core diameter can be determined by TEM, while SEC is capable of separating QDs based on the length of the capping agent (Figure 4b). As seen in Figure 4c), the hydrodynamic sizes obtained by SEC are consistent with the values calculated by adding the core diameter to the shell thickness values obtained from the literature.

Wang *et al.* [39] used SEC for separation of CdSe nanocrystals from the excess polymer (unbound poly(dimethylaminoethyl methacrylate) labeled with pyrene) used as coating material for nanocrystals. They were also able to quantify the amount of polymer that was bound to the nanocrystals. The polymer was analyzed by SEC at different concentrations and the peak areas of each run were recorded using a UV detector. For construction of a calibration curve for determination of polymer amounts, UV peak areas were plotted against concentration. This curve was used to determine the amount of free polymer (which was completely separated from the nanocrystal bound polymer) in a nanocrystal solution. Also, the amount of bound polymer (both concentration and average number of polymer chains bound to each CdSe particle) could be determined.

In addition to cadmium-based semiconductors, organic SEC has also been employed to characterize Pd nanocrystals [41], by focusing on the structure and stability of nanocrystals coated with alkanethiols of varying chain lengths. The hydrodynamic sizes of the nanocrystals were determined by calibrating the SEC column using polystyrene standards. The core diameters were determined by TEM.

As reported by many authors who have employed SEC for separation of NPs, analyte adsorption onto the SEC column packing material (induced by the high surface energy density of NPs) has been the most restricting factor contributing to the use of SEC in NP characterization. To overcome this problem, Arita *et al.* [40] synthesized a poly(methyl methacrylate) brush stationary phase immobilized onto silica which showed good column recovery (measured by comparing the DRI peak areas with and without the column) for CeO₂ NP and Qdot samples analyzed in THF. The separation performance was monitored by analyzing the eluted SEC fractions with TEM. The size-based separation was successful for both the CeO₂ NPs and the quantum dots. The experiments were successful in demonstrating the absence of strong interactions between the column packing material and the NPs and QDs.

5 Challenges and future prospects for SEC characterization of NPs and QDs. Comparison to other separation methods

As stated in the various literature references summarized in the section above, the most significant challenge in the SEC separation and characterization of NPs and QDs is their adsorption onto SEC stationary phases. A good laboratory practice in SEC is to measure (and report) column recovery, to assure that results are quantitative. Much to the contrary, however, column recoveries were reported in only one of the papers discussed in this review [30]. The reason behind this omission is probably the fact that quantitatively measuring NP and QD recovery from the column is not a straightforward task, due to difficulties related to the accurate determination of NP concentration in the eluate. It is well-known that UV-Vis spectroscopy can be used to determine concentration. If concentration is determined by measured absorbance, the molar absorptivity at the wavelength used needs to be known. However, molar absorptivity for metal NPs and QDs increases with increasing NP size [43] and, thus, a single value for molar absorptivity cannot be employed to calculate the population concentration in the UV-Vis peak of a disperse sample. Comparison of UV peaks can still be useful, however, by providing qualitative information on the recovery (*e.g.*, by comparing peak areas obtained using different concentrations of mobile phase modifier). While most spectroscopically-based detection methods (such as UV-Vis) fail with respect to determining the absolute concentration eluting from the column and, thus, quantifying column recovery, ICP-MS can be used for concentration determination by element-specific detection. Currently, the coupling of SEC to ICP-MS is rarely employed for the characterization of metal NPs and QDs [30, 44]. However, given the relative success with which other separation methods such as field-flow fractionation (FFF) [45] and hydrodynamic chromatography (HDC) [46–48] have been coupled to ICP-MS for the characterization of metal NPs, hyphenated SEC/ICP-MS experiments would appear to hold great potential in this respect [51–58].

SEC is generally, and most often, employed in the characterization of macromolecules, both synthetic and naturally occurring. Determination of molar mass (the molar mass distribution of a sample as well as its molar mass averages) is probably the most common application of SEC in polymer analysis. Molar mass can be determined by calibrating the columns using molar mass standards (ideally, with identical chemical composition and architecture as those of the polymer studied) or by using a static light scattering (SLS) detector together with concentration-sensitive detection (usually UV or DRI). Multi-angle static light scattering (MALS) detection can also be used for determination of size in the form of radius of gyration (R_G), a parameter which is usually more significant in NP characterization than is molar mass. Radius of gyration can be obtained from the angular dissymmetry of MALS data. There are, however, limitations in the use of SLS (including MALS) in NP characterization. Size from MALS cannot be determined for small particles ($\lesssim 10$ nm) such as QDs, because light scatters from small particles approximately equally at all angles and thus the angular dissymmetry needed for R_G determination is lacking (*i.e.*, QDs are near-isotropic scatterers). Additionally, metal NPs and QDs are strongly light absorbing and, consequently, weakly light scattering. This can affect the signal-to-noise ratio in light scattering when the total mass of injected NPs is low. Quasi-elastic light scattering (QELS),

which is also known as dynamic light scattering (DLS), can be used as an alternative to MALS in the determination of molecular size, in the form of R_H . The advantage of QELS over MALS is that QELS is capable of measuring sizes that are below 10 nm. QELS (as well as SLS) can be used both in off-line batch mode or on-line, coupled to separation techniques. To date, neither SLS nor QELS have been coupled to SEC to characterize metal NPs and QDs. As was the case for ICP-MS, however, both these detection techniques have been employed together with FFF for the size determination of separated NP species [52,56], such that coupling to SEC appears promising.

As regards other separation methods, analyte resolution in SEC is generally superior to that in flow FFF which, in turn, has generally better resolution than does HDC. The main reason for this relative ranking is the plate number N achievable by each separation method. While plate numbers in SEC experiments are much smaller than in techniques such as reversed-phase liquid chromatography, they are substantially larger than in flow FFF methods. (Within the family of flow FFF techniques, hollow-fiber flow FFF [47] achieves higher plate numbers than does asymmetric flow FFF [45,51–57] though, in both cases, N are much lower than in SEC). The ability to employ cross-flow gradients in flow FFF does mean that N in these methods is generally larger than in packed-column HDC, where the main parameter governing plate number is the size of the column packing particles. A thorough discussion of resolution in SEC can be found in references [9] and [10], while resolution in asymmetric flow FFF is discussed in reference [45] and resolution in HDC in reference [48]. SEC has also been found superior to both HDC and flow FFF with respect to analyte recovery, in the case of HDC due to column sorption issues, in FFF due to an open channel (or open fiber) design which generally precludes 100 % analyte recovery. An additional advantage of SEC and HDC over FFF is the need for specialized instrumentation and a large capital outlay to perform the latter, whereas the former employ instrumentation common to most liquid chromatography laboratories.

In an almost unique comparison among techniques, in 1981 Yau and Kirkland contrasted SEC and HDC to time-dependent exponential force-field sedimentation FFF for particle and ultra-high molar mass macromolecule analysis [59]. The authors found that this particular FFF method had a 5- to 10-fold better resolution than did SEC and a 10- to 50-fold better resolution than did packed-column HDC. For a discussion of how other separation techniques such as density gradient centrifugation and analytical centrifugation can be contrasted, at least in theory, to chromatographic and FFF methods, the reader is referred to chapters 6 and 8 of reference [60]. More recent discussions of analytical ultracentrifugation of nanoparticles are also given in references [61] and [62]. A novel nanoparticle characterization method was recently introduced, namely electrical asymmetrical flow FFF. The underlying principles and instrumentation, along with application examples, can be found in reference [63] and in the supporting information accompanying that paper.

6 Conclusions

Over the past 25 years, SEC has been employed to fractionate a variety of Au NPs, Ag NPs, and QDs. Because many NP and QD properties are size-dependent, a separation technique such as SEC is often needed to obtain NP populations with a narrow size distribution. SEC

experiments provides valuable information on the properties of NPs and QDs, including size, optical properties, and stability, and can also be employed for the purification of NP solutions. The most significant challenge in the SEC analyses of NPs and QDs, in both aqueous and organic solvents, is analyte adsorption onto the column stationary phase. Although some stationary phase/mobile phase combinations have been found to work better (less adsorption) than others, for most metal NPs and QDs the adsorption problem remains. Size information from SEC analyses has commonly been obtained by calibrating the columns with well-characterized standards. However, these results are not quantitative if adsorption occurs. Results can also be biased if reversible adsorption occurs, and/or other non-size-exclusion effects are present during the separation. At present, the door remains open for different detectors, such as SLS, QELS, and ICP-MS, to be used in conjunction with SEC to generate size information without column calibration, information on elemental profiles, and quantitation of column recoveries. The already successful coupling of these techniques, for the purposes of NP and QD characterization, to FFF and HDC, makes them both attractive and promising as SEC detectors for the types of analyses discussed in this review.

Acknowledgments

The Finnish Cultural Foundation is thanked for the financial support of L.P. through Foundations' Post Doc Pool. Commercial products are identified to specify adequately the experimental procedure. Such identification does not imply endorsement or recommendation by the National Institute of Standards and Technology, nor does it imply that the materials identified are necessarily the best available for the purpose.

Abbreviations

| | |
|---------------|--|
| CTAB | cetyltrimethylammonium bromide |
| DLS | dynamic light scattering |
| DRI | differential refractive index |
| FFF | field-flow fractionation |
| FL | fluorescence |
| HDC | hydrodynamic chromatography |
| ICP-MS | inductively coupled plasma mass spectrometry |
| LEDs | light-emitting diodes |
| MALS | multi-angle static light scattering |
| N | plate number |
| NPs | nanoparticles |
| PDA | photodiode array detector |
| PEG | polyethylene glycol |

| | |
|-------------------------|----------------------------------|
| QDs | quantum dots |
| QELS | quasi-elastic light scattering |
| R_G | radius of gyration |
| R_H | hydrodynamic radius |
| SDS | sodium dodecyl sulfate |
| SEC | size-exclusion chromatography |
| SLS | static light scattering |
| TEM | transmission electron microscopy |
| THF | tetrahydrofuran |
| UV-Vis | ultraviolet-visible |

References

1. Roduner E. Size matters: why nanomaterials are different. *Chem Soc Rev.* 2006; 35:583–592. [PubMed: 16791330]
2. Kreibig, U.; Vollmer, M. *Optical Properties of Metal Clusters.* Springer-Verlag; Heidelberg: 1995.
3. Deng W, Goldys EM. Chemical sensing with nanoparticles as optical reporters: from noble metal nanoparticles to quantum dots and upconverting nanoparticles. *Analyst.* 2014; 139:5321–5334. [PubMed: 25170528]
4. Kim C, Ghosh P, Rotello VM. Multimodal drug delivery using gold nanoparticles. *Nanoscale.* 2009; 1:61–67. [PubMed: 20644861]
5. Tran QH, Nguyen VQ, Le AT. Silver nanoparticles: synthesis, properties, toxicology, applications and perspective. *Adv Nat Sci: Nanosci Nanotechnol.* 2013; 4:033001/1–033001/20.
6. Kairdolf BA, Smith AM, Stokes TH, Wang MD, Young AN, Nie S. Semiconductor quantum dots for bioimaging and biodiagnostic applications. *Annu Rev Anal Chem.* 2013; 6:143–162.
7. Kim K, Han C, Jeong S. Design and synthesis of photostable multi-shell Cd-free nanocrystal quantum dots for LED applications. *J Mater Chem.* 2012; 22:21370–21372.
8. Huang H, Zhu J. The electrochemical applications of quantum dots. *Analyst.* 2013; 138:5855–5865. [PubMed: 23905161]
9. Striegel, AM.; Yau, WW.; Kirkland, JJ.; Bly, DD. *Modern Size-Exclusion Liquid Chromatography.* Second. Wiley; Hoboken, New Jersey: 2009.
10. Striegel, AM. *Liquid Chromatography: Fundamentals and Instrumentation.* Fanali, S.; Haddad, PR.; Poole, C.; Lloyd, P.; Schoenmakers, DK., editors. Elsevier; Amsterdam: 2013. p. 193-223.
11. Siebrands T, Giersig M, Mulvaney P, Fischer CH. Steric exclusion chromatography of nanometer-sized gold particles. *Langmuir.* 1993; 9:2297–2300.
12. Fischer CH, Giersig M. Analysis of colloids. VII. Wide-bore hydrodynamic chromatography, a simple method for the determination of particle size in the nanometer size regime. *J Chromatogr.* 1994; A 688:97–105.
13. Wilcoxon JP, Martin JE, Parsapour F, Wiedenman B, Kelley DF. Photoluminescence from nanosize gold clusters. *J Chem Phys.* 1998; 108:9137–9143.
14. Wei G, Liu F. Separation of nanometer gold particles by size exclusion chromatography. *J Chromatogr A.* 1999; 836:253–260.
15. Wei G, Liu F, Wang CRC. Shape separation of nanometer gold particles by size-exclusion chromatography. *Anal Chem.* 1999; 71:2085–2091. [PubMed: 21662743]

16. Liu F, Wei G. Effect of mobile-phase additives on separation of gold nanoparticles by size-exclusion chromatography. *Chromatographia*. 2004; 59:115–119.
17. Liu F. SEC characterization of Au nanoparticles prepared through seed-assisted synthesis. *Chromatographia*. 2007; 66:791.
18. Liu F. Monitoring the synthesis of Au nanoparticles using SEC. *Chromatographia*. 2008; 68:81–87.
19. Liu F, Chang Y. Using size-exclusion chromatography to evaluate changes in the sizes of Au and Au/Pd core/shell nanoparticles under thermal treatment. *Chromatographia*. 2011; 74:767–775.
20. Liu F. Using size-exclusion chromatography to monitor the stabilization of Au nanoparticles in the presence of salt and organic solvent. *Chromatographia*. 2012; 75:1099–1105.
21. Liu F. Using size-exclusion chromatography to monitor variations in the sizes of microwave-irradiated gold nanoparticles. *ISRN Chromatogr*. 2012:970685/1–970685/7.
22. Novak JP, Nickerson C, Franzen S, Feldheim DL. Purification of molecularly bridged metal nanoparticle arrays by centrifugation and size exclusion chromatography. *Anal Chem*. 2001; 73:5758–5761. [PubMed: 11774918]
23. Liu F. Analysis and applications of nanoparticles in the separation sciences: A case of gold nanoparticles. *J Chromatogr*. 2009; A 1216:9034–9047.
24. Liu F. Using SEC for analyzing the sizes of Au/Pt core/shell nanoparticles. *Chromatographia*. 2010; 72:473–480.
25. Fischer CH, Weller H, Katsikas L, Henglein A. Photochemistry of colloidal semiconductors. 30. HPLC investigation of small CdS particles. *Langmuir*. 1989; 5:429–432.
26. Fischer CH, Giersig M. Colloidal cadmium sulfide preparation via flow techniques: ultrasmall particles and the effect of a chromatographic column. *Langmuir*. 1992; 8:1475–1478.
27. Fischer CH, Giersig M, Siebrands T. V. Size-exclusion chromatography of colloidal semiconductor particles. *J Chromatogr*. 1994; A 670:89–97.
28. Fischer CH, Siebrands T. Analysis of colloids. VIII. Concentration- and memory effects in size exclusion chromatography of colloidal inorganic nanometer-particles. *J Chromatogr*. 1995; A 707:189–197.
29. Fischer CH, Kenndler E. Analysis of colloids. IX. Investigation of the electrical double layer of colloidal inorganic nanometer-particles by size-exclusion chromatography. *J Chromatogr*. 1997; A 773:179–187.
30. Trapiella-Alfonso L, Bustos AR Montoro, Encinar JR, Costa-Fernandez JM, Pereiro R, Sanz-Medel A. *Nanoscale*. 2011; 3:954–957. [PubMed: 21234505]
31. Wilcoxon JP, Martin JE, Provencio P. Size distributions of gold nanoclusters studied by liquid chromatography. *Langmuir*. 2000; 16:9912–9920.
32. Wilcoxon JP, Martin JE, Provencio P. Optical properties of gold and silver nanoclusters investigated by liquid chromatography. *J Chem Phys*. 2001; 115:998–1008.
33. Wilcoxon JP, Provencio P. Etching and aging effects in nanosize Au clusters investigated using high-resolution size-exclusion chromatography. *J Phys Chem B*. 2003; 107:12949–12957.
34. Wilcoxon JP, Provencio PP. Heterogeneous growth of metal clusters from solutions of seed nanoparticles. *J Am Chem Soc*. 2004; 126:6402–6408. [PubMed: 15149237]
35. Al-Somali AM, Krueger KM, Falkner JC, Colvin VL. Recycling size exclusion chromatography for the analysis and separation of nanocrystalline gold. *Anal Chem*. 2004; 76:5903–5910. [PubMed: 15456313]
36. Krueger KM, Al-Somali AM, Mejia M, Colvin VL. The hydrodynamic size of polymer stabilized nanocrystals. *Nanotechnology*. 2007; 18:475709/1–475709/7.
37. Wilcoxon JP, Provencio PP. Chemical and optical properties of CdSe and CdSe/ZnS nanocrystals investigated using high-performance liquid chromatography. *J Phys Chem*. 2005; B 109:13461–13471.
38. Krueger KM, Al-Somali AM, Falkner JC, Colvin VL. Characterization of nanocrystalline CdSe by size exclusion chromatography. *Anal Chem*. 2005; 77:3511–3515. [PubMed: 15924382]
39. Wang M, Dykstra TE, Lou X, Salvador MR, Scholes GD, Winnik MA. Colloidal CdSe nanocrystals passivated by a dye-labeled multidentate polymer: quantitative analysis by size-exclusion chromatography. *Angew Chem Int Ed*. 2006; 45:2221–2224.

40. Arita T, Yoshimura T, Adschiri T. Size exclusion chromatography of quantum dots by utilizing nanoparticle repelling surface of concentrated polymer brush. *Nanoscale*. 2010; 2:1467–1473. [PubMed: 20820736]
41. Murayama H, Narushima T, Negishi Y, Tsukuda T. Structures and stabilities of alkanethiolate monolayers on palladium clusters as studied by gel permeation chromatography. *J Phys Chem B*. 2004; 108:3496–3503.
42. Liu F. Monitoring stability and sizes of Au/Pd core/shell nanoparticles by SEC. *Chromatographia*. 2009; 70:7–13.
43. Yu WW, Qu L, Guo W, Peng X. Experimental determination of the extinction coefficient of CdTe, CdSe, and CdS nanocrystals. *Chem Mater*. 2003; 15:2854–2860.
44. L. Pitkänen, K.E. Murphy, A.R. Montoro Bustos, M.R. Winchester, A.M. Striegel. Manuscript in preparation.
45. Podzimek, S. Light scattering, size exclusion chromatography and asymmetric flow field flow fractionation. Wiley; Hoboken, New Jersey: 2011.
46. Brewer AK, Striegel AM. Characterizing a spheroidal nanocage drug delivery vesicle using multi-detector hydrodynamic chromatography. *Anal Bioanal Chem*. 2011; 399:1507–1514. [PubMed: 20711773]
47. Striegel AM. Hydrodynamic chromatography: packed columns, multiple detectors, and microcapillaries. *Anal Bioanal Chem*. 2012; 402:77–81. [PubMed: 21901463]
48. Striegel AM, Brewer AK. Hydrodynamic chromatography. *Annu Rev Anal Chem*. 2012; 5:15–34.
49. Pitkanen L, Striegel AM. Polysaccharide characterization by hollow-fiber flow field-flow fractionation with on-line multi-angle static light scattering and differential refractometry. *J Chromatogr A*. 2015; 1380:146–155. [PubMed: 25578045]
50. Pitkanen L, Striegel AM. AF4/MALS/QELS/DRI characterization of regular star polymers and their “span analogs”. *Analyst*. 2014; 139:5843–5851. [PubMed: 25221791]
51. Bolea E, Jimenez-Lamana J, Laborda F, Abad-Alvaro I, Blade C, Arola L, Castillo JR. Detection and characterization of silver nanoparticles and dissolved species of silver in culture medium and cells by AsFIFFF-UV-Vis-ICPMS: application to nanotoxicity tests. *Analyst*. 2014; 139:914–922. [PubMed: 24162133]
52. Gigault J, Hackley VA. Differentiation and characterization of isotopically modified silver nanoparticles in aqueous media using asymmetric-flow field flow fractionation coupled to optical detection and mass spectrometry. *Anal Chim Acta*. 2013; 763:57–66. [PubMed: 23340287]
53. Loeschner K, Navratilova J, Legros S, Wagner S, Grombe R, Snell J, von der Kammer F, Larsen EH. Optimization and evaluation of asymmetric flow field-flow fractionation of silver nanoparticles. *J Chromatogr A*. 2013; 1272:116–124. [PubMed: 23261297]
54. Bednar AJ, Poda AR, Mitrano DM, Kennedy AJ, Gray EP, Ranville JF, Hayes CA, Crocker FH, Steevens JA. Comparison of on-line detectors for field flow fractionation analysis of nanomaterials. *Talanta*. 2013; 104:140–148. [PubMed: 23597901]
55. Tiede K, Boxall ABA, Tiede D, Tear SP, David H, Lewis J. A robust size-characterization methodology for studying nanoparticle behaviour in real environmental samples, using hydrodynamic chromatography coupled to ICP-MS. *J Anal At Spectrom*. 2009; 24:964–972.
56. Cho TJ, Hackley VA. Fractionation and characterization of gold nanoparticles in aqueous solution: asymmetric-flow field flow fractionation with MALS, DLS, and UV-Vis detection. *Anal Bioanal Chem*. 2010; 398:2003–2018. [PubMed: 20803340]
57. Meerman B. Field-flow fractionation coupled to ICP-MS: separation at the nanoscale, previous and recent application trends. *Anal Bioanal Chem*. 2015; 407:2665–2674. [PubMed: 25577354]
58. Lewis DJ. Hydrodynamic chromatography – inductively coupled plasma mass spectrometry, with post-column injection capability for simultaneous determination of nanoparticle size, mass concentration and particle number concentration (HDC-PCI-ICP-MS). *Analyst*. 2015; 140:1624–1628. [PubMed: 25627965]
59. Yau WW, Kirkland JJ. Comparison of sedimentation field flow fractionation with chromatographic methods for particulate and high-molecular-weight macromolecular characterizations. *J Chromatogr*. 1981; 218:217–238.
60. Giddings, JC. Unified separation science. Wiley-Interscience; New York: 1991.

61. Mächtle, W.; Börger, L. Analytical ultracentrifugation of polymers and nanoparticles. Springer; Berlin: 2006.
62. Mittal V, Völkel A, Cölfen H. Analytical ultracentrifugation of model nanoparticles: Comparison of different analysis methods. *Macromol Biosci.* 2010; 10:754–762. [PubMed: 20480509]
63. Johann C, Elsenberg S, Schuch H, Rösch U. Instrument and method to determine the electrophoretic mobility of nanoparticles and proteins by combining electrical and flow field-flow fractionation. *Anal Chem.* 2015; 87:4292–4298. [PubMed: 25789885]

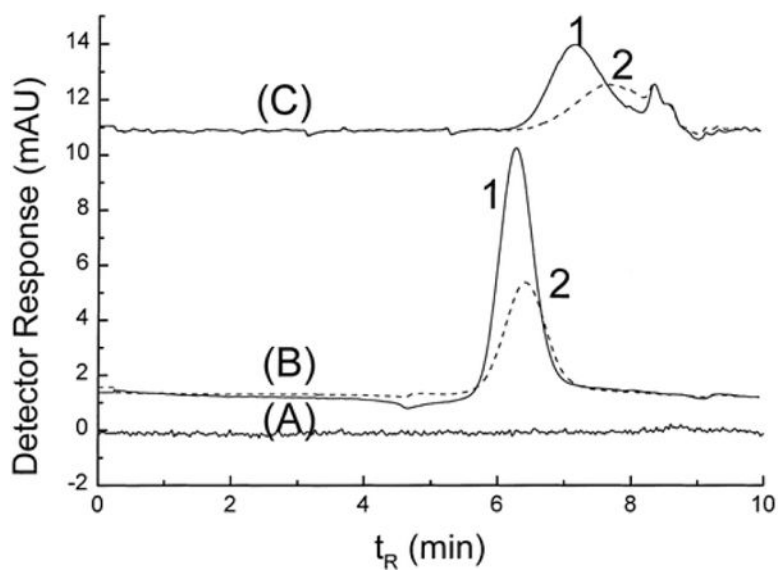


Figure 1. Effect of mobile phase additives on the SEC separation of AuNPs with different shapes (nanorods, detected at $\lambda_0 = 920$ nm, solid line (1) in the chromatogram, and spherical, detected at $\lambda_0 = 520$ nm, dashed line (2) in the chromatogram). (A) H_2O , (B) 40 mmol L^{-1} SDS, and (C) 40 mmol L^{-1} SDS and 30 mmol L^{-1} Brij-35. Reprinted with permission from reference [15].

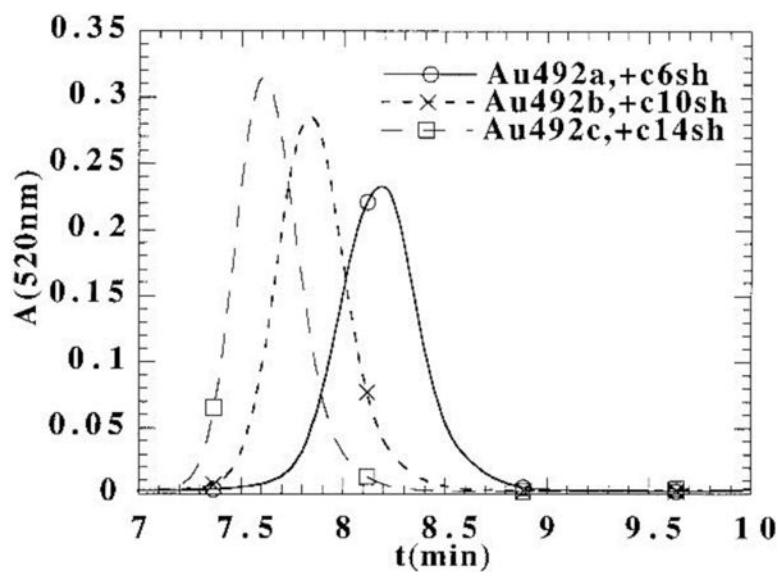


Figure 2. Effect of alkylthiol capping agents (C_6SH , $C_{10}SH$, $C_{14}SH$) on the SEC retention time of Au nanoclusters. The absorbance at 520 nm from the PDA versus elution time is shown. The size of the clusters was obtained by calibrating the column with polystyrene standards. Reprinted with permission from reference [31].

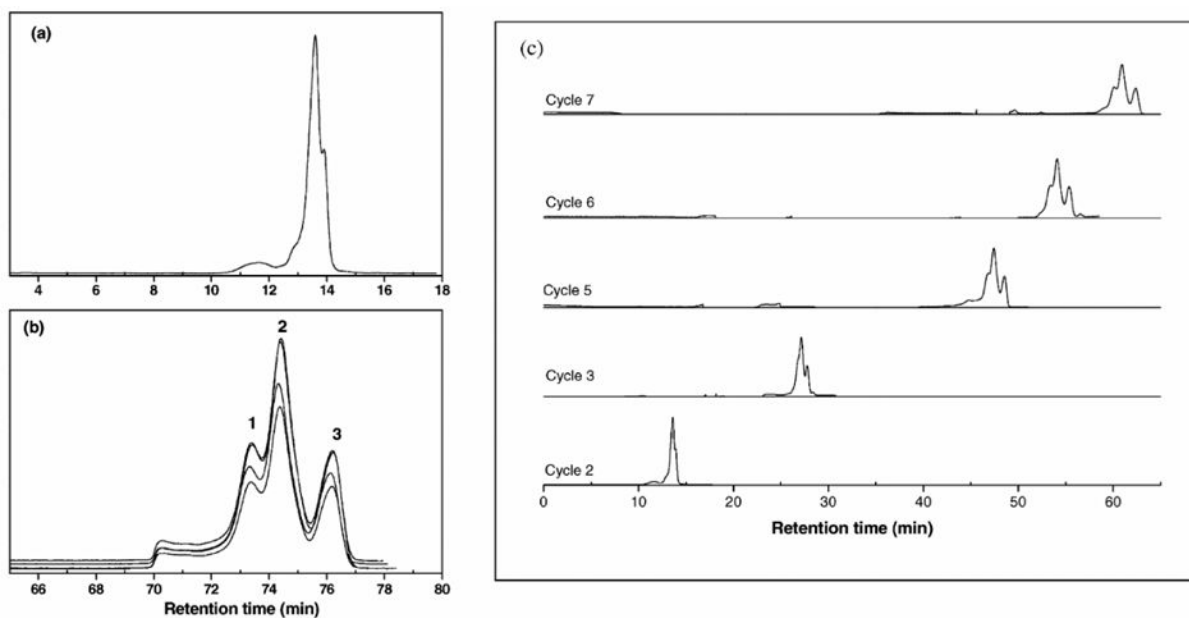


Figure 3. Alternate-recycling SEC chromatograms of a broadly dispersed Au NP sample. (a) A chromatogram of cycle 2, (b) four overlaid chromatograms of cycle 8, and (c) the evolution of the data as a function of cycle number. Reprinted with permission from reference [35].

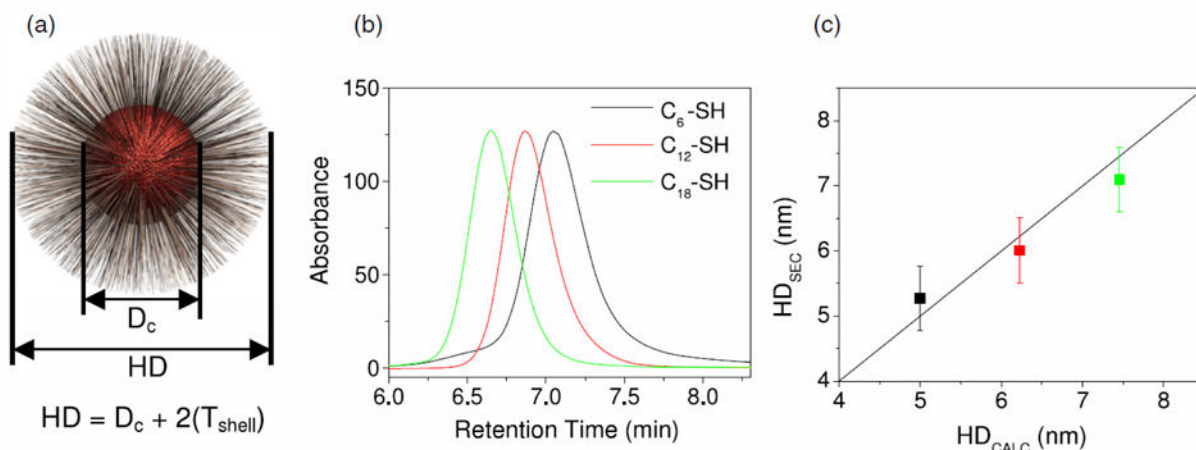


Figure 4.

Geometric model of total hydrodynamic diameter (HD) of NP. (a) The HD is calculated from core diameter (D_c) and surface-coating thickness (T_{shell}). (b) SEC detects the retention time difference in capping agent length between CdSe nanoparticles coated with 1-hexane (C_6), 1-dodecane (C_{12}), and 1-octadecane (C_{18}) thiol (SH). (c) The hydrodynamic diameter of the coated NPs determined from SEC (HD_{SEC}) is compared to expected values for 3.6 nm CdSe core plus literature values for the shell thickness (HD_{CALC}). The line slope is set to 1. Reprinted with permission from reference [36].

Table 1

SEC methodology used for separation and characterization of metal NPs and QDs.

| Metal nanoparticle (stabilizer/capping agent) | SEC column(s) | Eluent | Detection | Column calibration standard for size determination | Remarks | Reference(s) |
|---|---|--|--|---|---|--------------|
| SEC in aqueous solution | | | | | | |
| Au (citrate) | Nucleosil 500 + Nucleosil 1000 C4 (Machery-Nagel) | 10 ⁻³ mol L ⁻¹ sodium citrate | PDA | Synthesized Au NPs (diameter determined by TEM) | | [11] |
| Au (citrate) | Nucleosil 500 + Nucleosil 1000 C4 (Machery-Nagel) | 10 ⁻³ mol L ⁻¹ sodium citrate | PDA | Commercial PEG, polysaccharides | SEC used for separation of AuNPs from impurities prior investigation of AuNP photoluminescence | [12] |
| Au (citrate) | TSK3000 (Toyo) | H ₂ O | UV-Vis ($\lambda_0 = 525$ nm) and FL ($\lambda_{em} = 440$ nm, $\lambda_{exc} = 230$ nm) | Commercial Au NPs (diameter determined by the manufacturer) | 5 mmol L ⁻¹ SDS authors' choice from the tested mobile phases (used also when calibrating the column) | [13] |
| Au (citrate) | Nucleogel GFC 1000-8 (Machery-Nagel) | H ₂ O, 0.1 mmol L ⁻¹ SDS, 1 mmol L ⁻¹ SDS, 5 mmol L ⁻¹ SDS, 80 mmol L ⁻¹ SDS | PDA | Commercial Au NPs (diameter determined by the manufacturer) | 40 mmol L ⁻¹ SDS + 30 mmol L ⁻¹ Brij-35 gave best resolution when separating spherical and rod-shaped AuNPs | [14] |
| Spherical and rod-shaped Au (CTAB) | Nucleogel GFC 1000-8 (Machery-Nagel) | H ₂ O, 40 mmol L ⁻¹ SDS, 40 mmol L ⁻¹ SDS + 30 mmol L ⁻¹ Brij-35 | PDA | Commercial AuNPs (diameter determined by the manufacturer) | The adsorption of AuNPs on C ₁₈ -capped silica gel was found in separate TEM studies | [15] |
| Au (citrate) | Nucleosil, 100 nm pore size and 7 μ m particle size (Machery-Nagel) | 5 mmol L ⁻¹ sodium citrate, 20 mmol L ⁻¹ sodium citrate, NaCl (concentrations used not reported), 15 mmol L ⁻¹ SDS, 50 mmol L ⁻¹ SDS | UV-Vis ($\lambda_0 = 520$ nm) | Commercial AuNPs (diameter determined by the manufacturer) | | [16] |
| Au (citrate) | Nucleogel GFC 60-8 (Machery-Nagel) | 10 mmol L ⁻¹ SDS | UV-Vis ($\lambda_0 = 520$ nm) | Commercial AuNPs (diameter determined by the manufacturer) | | [17-21] |
| Phenylethynyl-bridged AuNP dimers and trimers (citrate) | Silica microsphere GPC columns, 500 Å and 350 Å (Alltech, Inc.) | 40 mmol L ⁻¹ SDS | UV-Vis ($\lambda_0 = 525$ nm) | Commercial AuNPs (diameter determined by the manufacturer) | | [22] |
| Au/Pd core/shell (SDS) | Nucleogel GFC 60-8 (Machery-Nagel) | 10 mmol L ⁻¹ SDS | UV-Vis ($\lambda_0 = 520$ nm) | Commercial AuNPs (diameter determined by the manufacturer) | | [19,23] |
| Au/Pt core/shell (SDS) | Nucleogel GFC 60-8 (Machery-Nagel) | 10 mmol L ⁻¹ SDS | UV-Vis ($\lambda_0 = 520$ nm) | Commercial AuNPs (diameter determined by the manufacturer) | | [24] |

| Metal nanoparticle (stabilizer/capping agent) | SEC column(s) | Eluent | Detection | Column calibration standard for size determination | Remarks | Reference(s) |
|---|--|--|---|--|--|--------------|
| CdS (polyphosphate) | Nucleosil 500 C4 + Nucleosil 1000 C4 (Machery-Nagel) | 10^{-3} mol L ⁻¹ Cd(ClO ₄) ₂ + 10^{-3} mol L ⁻¹ hexametaphosphate | PDA | Narrow dispersity CdS (diameter determined by TEM) | | [12,25–29] |
| ZnS (polyphosphate) | Nucleosil 500 C4 + Nucleosil 1000 C4 (Machery-Nagel) | 10^{-3} mol L ⁻¹ Zn(ClO ₄) ₂ + 10^{-3} mol L ⁻¹ hexametaphosphate | PDA | Narrow dispersity ZnS (diameter determined by TEM) | | [27] |
| CdSe (amphiphilic polymer) | Superdex 200 (GE Healthcare Life Sciences) | 0.1 mol L ⁻¹ NH ₄ HCO ₃ , pH 7.4 | UV-Vis, FL, ICP-MS | | Column recoveries reported | [30] |
| CdSe/ZnS core/shell (amphiphilic polymer) | Superdex 200 (GE Healthcare Life Sciences) | 0.1 mol L ⁻¹ NH ₄ HCO ₃ , pH 7.4 | UV-Vis, FL, ICP-MS | | Column recoveries reported | [30] |
| SEC in organic solvent | | | | | | |
| Au (octane/tridodecylmethylammonium chloride/hexanol) | PL-500 (Agilent/Polymer Laboratories) | THF | PDA ($\lambda_0 = 520$ nm) and FL ($\lambda_0 = 520$ nm, ex = 300 nm) | | | [13] |
| Au (various alkylthiols) | PL-1000 or PL-500 (Agilent/Polymer Laboratories) | 0.01 mol L ⁻¹ dodecanethiol in toluene | PDA ($\lambda_0 = 520$ nm), DRI, conductivity | Linear alkanes and polystyrene standards | DRI and conductivity detection used to demonstrate that AuNPs had no charge and that AuNPs were separated from the nonabsorbing chemicals | [31–34] |
| Au (octadecanethiol/tetraoctanethiol/decanethiol) | PL-gel 1110 (Agilent/Polymer Laboratories) | Toluene | UV-Vis ($\lambda_0 = 520$ nm), DRI | Polymer standards (not specified) | Recycling SEC used in addition to conventional SEC | [35] |
| Au (polystyrene coated) | PL-gel 1110 (Agilent/Polymer Laboratories) | Toluene | PDA ($\lambda_0 = 505$ nm), DRI | Polystyrene standards | | [36] |
| Ag (tetraoctylammonium bromide/tetraoctylammonium chloride/trioctylphosphine) | PL-1000 (Agilent/Polymer Laboratories) | 0.01 mol L ⁻¹ dodecane thiol in toluene | PDA ($\lambda_0 = 400$ nm), DRI, conductivity | Linear alkanes and polystyrene standards | DRI and conductivity detection used to demonstrate that AgNPs had no charge and that AgNPs were separated from the non-absorbing chemicals | [32] |
| CdS (dodecanethiol) | Nucleosil 500 + Nucleosil 1000 (Machery-Nagel) | 1 mmol L ⁻¹ Cd(ClO ₄) ₂ + 1 mmol L ⁻¹ dodecanethiol in THF | PDA | | | [27] |
| CdSe (alkylphosphines) | PL-50 or PL-1000 (Agilent/Polymer Laboratories) | THF | PDA, DRI, FL | | DRI was used to detect non-absorbing chemicals | [37] |
| CdSe (alkylthiols) | PL-gel 1110 (Agilent/Polymer Laboratories) | 0.1 mol L ⁻¹ trioctylphosphine in toluene | UV-Vis | Polystyrene standards | Recycling SEC used in addition to conventional SEC | [38] |
| CdSe with a ligand of poly(dimethylaminoethyl methacrylate) labeled with pyrene | AM Gel Linear/5 (American Polymer Standards Corporation) | N-methyl-2-pyrrolidinone | UV-Vis ($\lambda_0 = 343$ nm), DRI | | | [39] |

| Metal nanoparticle (stabilizer/capping agent) | SEC column(s) | Eluent | Detection | Column calibration standard for size determination | Remarks | Reference(s) |
|--|---|--|----------------------------------|--|--|--------------|
| Polystyrene coated CdSe | PLgel 1110 (Agilent/Polymer Laboratories) | 0.1 mol L ⁻¹ trioctylphosphine in toluene | PDA ($\lambda_0 = 517$ nm), DRI | Polystyrene standards | | [36] |
| CdSe/ZnS core/shell (alkylphosphines) | PL-50 or PL-1000 (Agilent/Polymer Laboratories) | THF | PDA, DRI, FL | | DRI was used to detect non-absorbing chemicals | [37] |
| CeO ₂ (unmodified and surface modified) | poly(methyl methacrylate brush immobilized silica monolith columns; Shodex KF-803L and Shodex KF-805L | THF | DRI | | poly(methyl methacrylate brush stationary phase was synthesized by authors | [40] |
| Pd (dodecanethiol/dodecanethiol/hexadecanethiol) | JAIGEL-W253 (Japan Analytical Industry Co., Ltd) | Toluene | UV-Vis ($\lambda_0 = 290$ nm) | Polystyrene standards | Recycling preparative SEC | [41] |
| Qdot® 545 and 705 | poly(methyl methacrylate brush immobilized silica monolith columns; Shodex KF-803L and Shodex KF-805L | THF | DRI | | poly(methyl methacrylate brush stationary phase was synthesized by authors Qdot 545 is CdSe/ZnS (core/shell) and Qdot 705 is CdSe Te/ZnS (core/shell) | [40] |